Astronomy
&
Astrophysics

First results from the IBIS/ISGRI data obtained during the Galactic Plane Scan[*]

II. The Vela region

J. Rodriguez[1,2], M. Del Santo[3], F. Lebrun[4], G. Belanger[4], M. Cadolle-Bel[4] F. Capitanio[3], P. David[1], L. Foschini[5], P. Goldoni[4], A. Goldwurm[4], A. Gros[4], P. Laurent[4], A. Paizis[6,2], J. Paul[4], R. Terrier[1], S. E. Shaw[7,2], and P. Ubertini[3]

[1] CEA Saclay, DSM/DAPNIA/SAp (CNRS FRE 2591), 91191 Gif-sur-Yvette Cedex, France
[2] Integral Science Data Center, Chemin d'Écogia, 16, 1290 Versoix, Switzerland
[3] IASF/CNR, via del Fosso del Cavaliere 100, 00133 Roma, Italy
[4] CEA Saclay, DSM/DAPNIA/SAp, 91191 Gif-sur-Yvette Cedex, France
[5] IASF/CNR, sezione di Bologna, via Gobetti 101, 40129 Bologna, Italy
[6] IASF/CNR, Sezione di Milano, via Bassini 15, 20133 Milano, Italy
[7] School of Physics and Astronomy, University of Southampton, Southampton, SO17 1BJ UK

Abstract. We report on INTEGRAL/IBIS observations of the Vela region during a Galactic Plane Scan (hereafter GPS) presenting the IBIS in-flight performances during these operations. Among all the known sources in the field of view we clearly detect 4U 0836−429, Vela X−1, Cen X−3, GX 301−2, 1E 1145.1−6141, and H0918−549 in the 20−40 keV energy range. Only Vela X−1 and GX 301−2 are detected in the 40−80 keV energy range, and no sources are visible above. We present the results of each individual observation (∼2200 s exposure), as well as those from the mosaic of these scans.

Key words. instrumentation: detectors – Galaxy: disk – γ-rays: observations – X-rays: binaries

1. Introduction

The IBIS telescope (Ubertini et al. 2003) on board the INTEGRAL observatory is a γ-ray sensitive coded mask telescope. It is composed of two layers, each one being a detector. The upper one, ISGRI (Lebrun et al. 2003), is sensitive between 15 keV and 1 MeV, and is optimized between 15 keV and ∼200 keV. The lower one, PICSIT (Di Cocco et al. 2003), is sensitive between ∼175 keV and ∼10 MeV. Due to its high angular resolution (12′ FWHM), and wide field of view (FOV, 19° × 19° at half response) IBIS is perfectly suited for the discovery and localisation of new transient X-ray and γ-ray sources. The energy range and the high sensitivity of ISGRI are particularly well adapted to perform a hard X-ray survey of the Galactic plane. In order to exploit these features ∼8% of the observing time is devoted to scans of the Galactic plane (GPS)

during the first year of the nominal mission. For a precise description of the GPS see Winkler et al. (2003).

Such scans are particularly important to follow up transient and persistent X-ray sources, and for the discovery of new X-ray novæ. Up to now, more than 10 hard X-ray sources have been (re-)discovered mainly with the ISGRI layer of the IBIS detector. The INTEGRAL observations of the first such source, IGR J16318−4848 (Courvoisier et al. 2003), are presented by Walter et al. (2003a). Most of these sources belong to the class of X-ray binaries (XB), accretion powered binary systems that host a compact object (neutron star or black hole), and that can be persistent or transient. X-ray transients (XT) spend most of their life in quiescence, and are detected in the X-rays as they undergo episodes of outburst. These outbursts can be recurrent (e.g. 4U 1630−47, XTE J1550−564) or only detected once (Nova Musca 1991). Persistent sources are always visible in X and γ-rays (e.g. Cyg X−1, or GX 339−4). In the former case, ISGRI's sensitivity allows the detection of an outburst well before the other all-sky monitors, especially for outbursts starting with periods of hard states (e.g. XTE J1550−564, Dubath et al. 2003), but also for investigating the late stages of outbursts, that are poorly studied in this spectral range up to now (e.g. XTE J1720−318, Goldoni et al. 2003). The IBIS spectral range is also particularly well suited to discover,
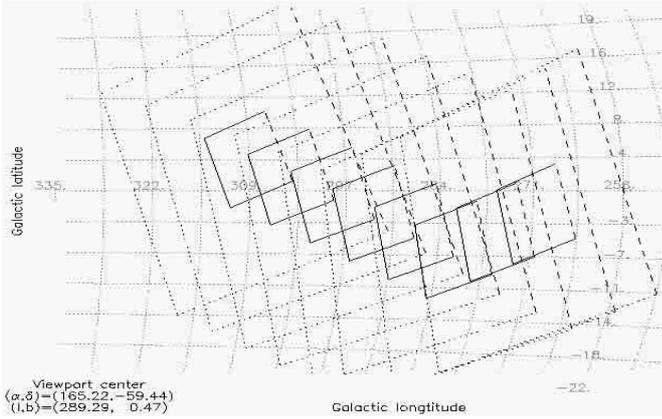

Fig. 1. Scheme of the GPS performed during Rev. 30. The scan started at $l = 270.0°$ and finished at $l = 309.5°$. The continuous squares represent the limits of the fully coded field of view, and the dashed squares the limit of the partially coded field of view.

or re-discover heavily absorbed sources, which were missed during previous observations in the soft (1−10 keV) band, where the X-rays are very sensitive to the absorption along the line of sight. The high localisation accuracy of INTEGRAL's imaging software (∼1′, Gros et al. 2003) and the understanding of the alignment systematics (Walter et al. 2003b) have already allowed for three multiwavelength counterpart searches and/or follow-up observations in softer X-rays with high sensitivity X-ray telescopes such as XMM-Newton (IGR J16318−4848, Matt & Guainazzi 2003; IGR J16320−4751, Rodriguez et al. 2003), and Chandra (IGR J16358−4726 Kouveliotou et al. 2003). Such multiwavelength observations are the best tool for identifying the nature of a source.

Other types of sources are also known to produce significant X-ray and γ-ray emission: anomalous X-ray pulsars, isolated pulsars, AGN seen through the Galactic plane, and high energy sources such as those detected by the EGRET telescope. The unprecedented localisation accuracy of IBIS over its energy domain will without a doubt help in identifying some of the so-called "unidentified" EGRET sources, as well as their possible X- and γ-ray counterparts several of which are often found within EGRET's large error box.

After a first scan in the Cygnus region (Del Santo et al. 2003, hereafter Paper I), where the telescope has demonstrated its ability in imaging bright sources like Cyg X−1, a second scan was performed on the other side of the Galactic plane, starting on the Vela region and finishing around the Centaurus region. We present here the results obtained during these observations, where many fainter sources are detected. Technical aspects of the observations and data reduction method are presented in the following section. The results are presented in Sect. 3 and discussed in Sect. 4.

2. Observations and data reduction

The GPS considered here was carried out on January 11th 2003, it is composed of 8×2200 s pointings. The scan started at 11h51 UTC, and finished at 17h35 UTC. The first individual observation was centered on $l = 270.0°$, and the last one

Table 1. Log of the observations performed during the scan.

Obs. Number	time	Pointing direction	
	(UTC)	RA	Dec
1	11h51	$09^h02^m27.22^s$	$-49°47'52.7''$
2	12h57	$09^h17^m12.99^s$	$-55°20'58.0''$
3	13h37	$09^h37^m06.03^s$	$-60°47'39.5''$
4	14h17	$10^h25^m34.76^s$	$-62°32'12.4''$
5	14h58	$11^h18^m36.64^s$	$-63°09'17.5''$
6	15h38	$12^h10^m57.27^s$	$-62°30'19.5''$
7	16h18	$12^h59^m12.47^s$	$-60°42'38.2''$
8	16h58	$13^h41^m07.60^s$	$-57°57'48.4''$

on $l = 309.5°$ (Fig. 1). The log of the observations is shown in Table 1.

The images were generated with the standard pipeline developed in cooperation by CEA/Saclay and ISDC/Versoix (see e.g. Goldwurm et al. 2001, 2003). For each pointing we have produced images in 3 energy ranges, 20−40 keV, 40−80 keV, 80−160 keV. Note that PICsIT works in a higher energy range (above 200 keV), where very long exposures (10^5–10^6 s) are required to obtain significant detections. PICsIT data are not considered further in this analysis. All the pointings were then combined to produce a mosaic. The image analysis is performed in a way such that the positions of all detected excesses are compared to catalog (Ebisawa et al. 2003) source positions and then fitted to obtain a fine position (Goldwurm et al. 2001, 2003). Any excess whose position does not correspond to a catalog source is labeled as a new source. No such new source was found in our analysis. Only sources with a significance level greater than 5 and for which the fitting procedure converged are considered in this paper.

3. Results

The 20−40 keV images obtained for some individual pointings are presented in Fig. 2, and the 20−40 keV mosaic produced from the whole scan in Fig. 3.

The scientific parameters such as the source position and the flux returned from the software are reported in Table 2. For each of them we estimate the offset between the position found with ISGRI and the catalogue (based on the SIMBAD database) position. The angle from the center of the FOV is also reported. It is clear that a precise analysis of a given GPS requires that each pointing is precisely studied along with the mosaic resulting from the summation of all pointings. Variable sources can appear in unique pointings, and be absent in the following ones, and therefore not be detected in a mosaic because the S/N is less than for the pointing where the source is bright. This is probably the case for H0918−549 and 4U 0836−429, both variable sources. Note that 4U 0836−429 can only be seen in two pointings, and that it is at the edge of the FOV (where the sensitivity is much lower) in the second one, which can also explain why it is detected only in the first pointing. On the other
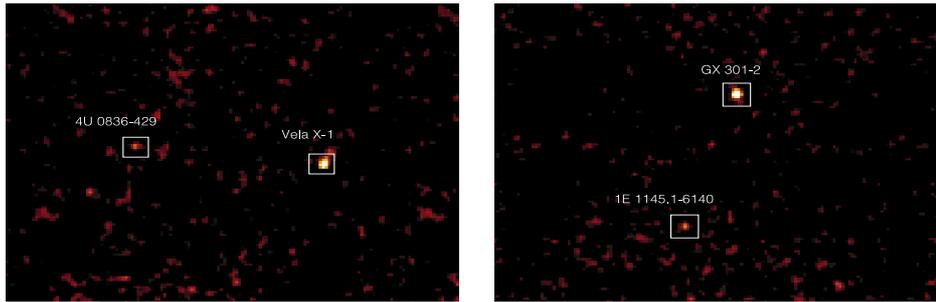
Fig. 2. 12.6 × 10° zoom on the individual 20−40 keV image from obs #1, and #6. This sequence illustrates the sensitivity achieved in individual pointings. GX 301−2, Vela X−1, 4U 0836−429, 1E 1145.1−6141 are clearly detected by the software. 4U 0836−429, is not detected in the mosaic. Note that there are still some residuals/background structures in the images. The precise background correction is discussed in Terrier et al. (2003).
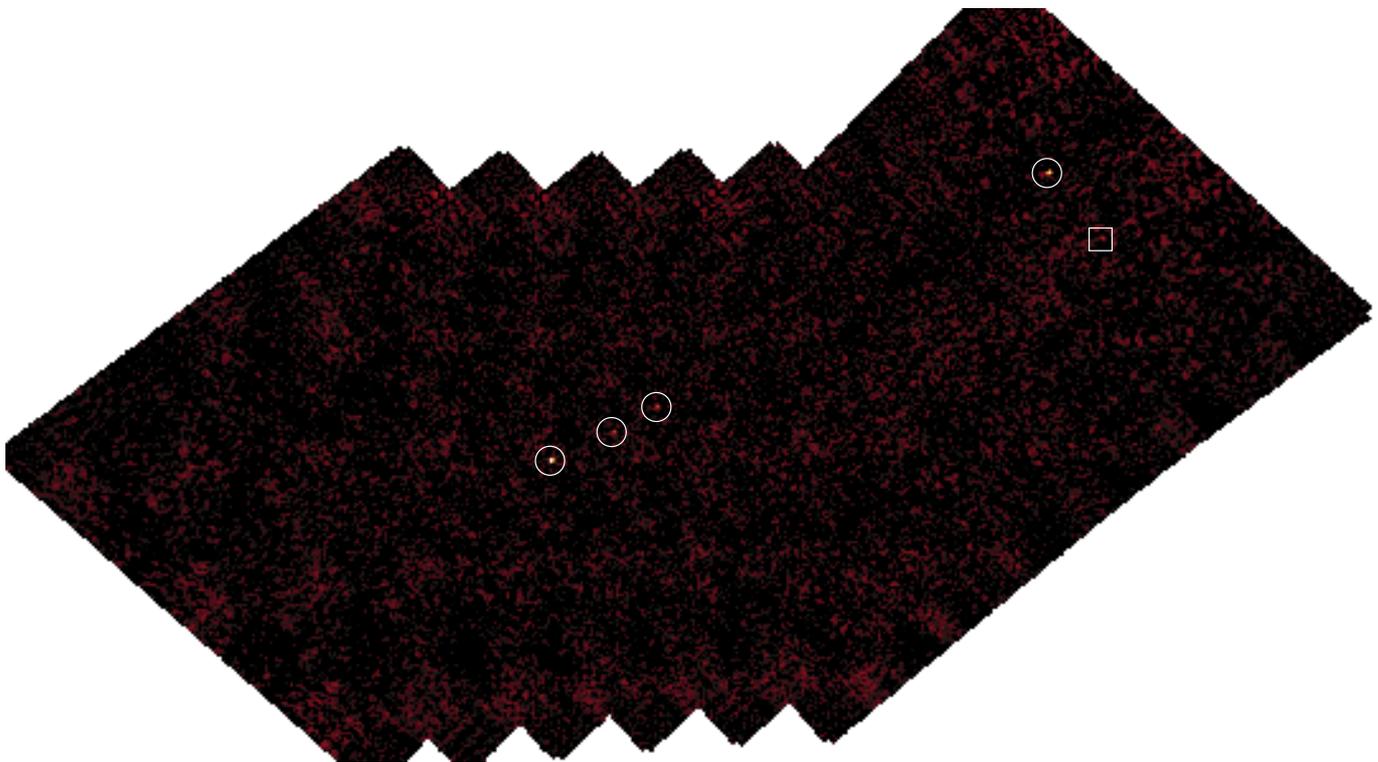

Fig. 3. 20−40 keV mosaic image produced by summing each individual image. Four sources are detected by the software (circles), from right to left these are Vela X−1 Cen X−3, 1E 1145.1−6141, and GX 301−2. Although not detected 4U0836−429 (square) is visible on the image.

hand, steady faint sources will not appear in a single pointing, but need more accumulation time to be detected.

4. Discussion

From the analysis of each individual pointing, sources with a relatively low level of flux (∼20 mCrab in the 20−40 keV energy range) have been detected with a relatively good accuracy on the estimated position (1.8′ offset for H0918−549 Table 2). This level of flux seems to be the sensitivity limit of ISGRI at the current stage of development[1] (see also Paper I). Note that for large angles from the center of the FOV, the flux of a source is still rather uncertain at this early stage of the mission. Fainter sources can be detected with longer exposure

times, as e.g. 1E1145.1−6141, which, has an averaged flux of about 20 mCrab, over the four pointings where it is in the FOV. Some slight offset (up to 3.5′) is still found between the estimated positions and the catalogue ones. It is worth noting that the offset depends on two factors: the distance from the center of the FOV, and the source flux (thus the significance of its detection). As the source is far from the centre, the off-set increases (Table 2), while for bright sources (sources detected with higher significance) the location accuracy usually increases (see Gros et al. 2003; Walter et al. 2003b and Paper I). In the 40−80 keV energy range only Vela X−1 and GX 301−4 are detected, and no source is seen above.

One important aspect of such scans is that they allow source evolution to be followed on long time scales. As mentioned in the introduction, they enable transient source to be detected as

[1] ∼5σ detection level for an exposure of 2200 s.

Table 2. Scientific parameters returned by the software; position (after having applied the misalignment matrix, Walter et al. 2003b) and flux of the detected sources in the 20−40 keV energy range, for each individual pointing, and the final mosaic. We have put in addition the offset between the estimated position, and the real position as given by the SIMBAD online archives. The off axis angle is also given for each pointing. The source types are extracted from the catalogues of Liu et al. (2000, 2001).

Source	Type	Flux (mCrab)	offset (arcmin)	offaxis angle
Pointing No. 1				
Vela X−1	HMXB	79 ± 5	2.3	9.2°
4U 0836−429	LMXB	38 ± 6	2.7	8.0°
Pointing No. 2				
H0918−549	LMXB	21 ± 4	1.8	29 arcmin
Pointing No. 4				
Cen X−3	HMXB	32 ± 5	2.7	6.9°
GX 301−2	HMXB	59 ± 9	2.9	13.8°
Pointing No. 5				
Cen X−3	HMXB	32 ± 4	1.0	2.5°
GX 301−2	HMXB	53 ± 5	0.6	7.7°
Pointing No. 6				
GX 301−2	HMXB	75 ± 4	0.7	1.8°
1145.1−6141	HMXB	30 ± 5	1.6	2.8°
Pointing No. 7				
GX 301−2	HMXB	76 ± 5	1.1	4.3°
1145.1−6141	HMXB	22 ± 4	0.2	8.6°
Pointing No. 8				
GX 301−2	HMXB	70 ± 5	3.5	10.3°
Result of the mosaic				
Source Name		Flux mCrab		offset arcmin
Vela X−1		91 ± 7		2.4
GX 301−2		71 ± 4		0.8
Cen X−3		27 ± 3		2.2
1145.1−6141		20 ± 3		2.0

they undergo outbursts. However, as illustrated here in the particular case of GX 301−2, and thanks to the large FOV of the IBIS detector, such scans are particularly important to construct light curves of persistent sources, during the time they are seen in the FOV of the telescope. By repeating those GPS patterns from time to time, it is possible to monitor the long term behaviour of those sources.

The ISGRI camera of the IBIS detector onboard INTEGRAL has largely proven its utility in such scans, after only ~6 months of activity. Many of the new sources found up to now were detected during scans of the Galactic plane or of the Galactic Center region. With its high positioning accuracy it allowed for the identification of counterparts, and for X-ray follow-up (Revnivtsev et al. 2003; Rodriguez et al. 2003). It appears thus as an instrument of primary importance in multi-wavelength campaigns dedicated to the study of sources of high energy, which are the only valuable way to understand properly the physical mechanisms in action in those sources.

References

Courvoisier, T., Walter, R., Rodriguez, J., et al. 2003, IAUC, 8063
Del Santo, M., Rodriguez, J., Ubertini, P., et al. 2003, A&A, 411, L369
Di Cocco, G., Caroli, E., Celesti, E., et al. 2003, A&A, 411, L189
Dubath, P., Revnivtsev, M., Goldoni, P., et al. 2003, IAUC, 8100
Ebisawa, K., Bourban, G., Bodaghee, A., et al. 2003, A&A, 411, L59
Goldoni, P., Goldwurm, A., Kuulkers, E., et al. 2003, Atel, 153
Goldwurm, A., Goldoni, P., Gros, A., et al. 2001, Proc. of the 4th INTEGRAL Workshop, ed. A. Gimenez, V. Reglero, & C. Winkler
Goldwurm, A., David, P., Foschini, L., et al. 2003, A&A, 411, L223
Gros, A., Goldwurm, A., Cadolle-Bel, M., et al. 2003, A&A, 411, L179
Kouveliotou, C., Patel, S., Tennant, A., et al. 2003, IAUC, 8109
Lebrun, F., Leray, J. P., Lavocat, P., et al. 2003, A&A, 411, L141
Liu, Q. Z., van Paradijs, J., & van den Heuvel, E. P. J. 2000, A&AS, 147, 25
Liu, Q. Z., van Paradijs, J., & van den Heuvel, E. P. 2001, A&A, 368, 1021
Matt, G., & Guainazzi, M. 2003, MNRAS, 341, L13
Rodriguez, J., Tomsick, J. A., Foschini, L., et al. 2003, A&A, 407, L41
Terrier, R., Lebrun, F., Sauvageon, A., et al. 2003, A&A, 411, L167
Ubertini, P., Lebrun, F., Di Cocco, G., et al. 2003, A&A, 411, L131
Walter, R., Rodriguez, J., Foschini, L., et al. 2003a, A&A, 411, L427
Walter, R., Favre, P., Dubath, P., et al. 2003b, A&A, 411, L25
Winkler, C., Gehrels, N., Schöenfelder, V., et al. 2003, A&A, 411, L349